Key Intermediate Product of Oxidative Degradation of Photochromic Spirooxazines. X-ray Crystal Structure and Electron Spin Resonance Analysis of Its 7,7,8,8-Tetracyanoquinodimethane Ion-Radical Salt†

Vincenzo Malatesta,*,‡,§ Roberto Millini,⊥ and Luciano Montanari⊥

Contribution from Enichem Synthesis, Via Maritano 26, 20097 S. Donato (MI), Italy, and Eniricerche, Via Maritano 26, 20097 S. Donato (MI), Italy

Received July 6, 1994⊗

Abstract: The preparation and characterization of the 7,7,8,8-tetracyanoquinodimethane (TCNQ) ion-radical salt of the key oxidation product of the photochromic spirooxazines are described. This salt is prepared through a thermal oxidation reaction of TCNQ on spirooxazines. X-ray diffraction analysis shows it to be a complex salt, consisting of neutral TCNQ, $TCNQ^{\bullet-}$ radical anion, and a rearranged oxidized product of spirooxazine (nominal 1:1:1 stoichiometry), which crystallizes in the monoclinic space group $P2_1/c$ with $a = 17.014(3)$ Å, $b = 25.912(5)$ Å, $c = 8.809(1)$ Å, $\beta = 90.18(1)°$, $V = 3883.6(11)$ Å^3, and $D_{calcd} = 1.3064$ Mg/m^3 for $Z = 4$. Least-squares refinement of the model based on 4321 reflections ($I > 3\sigma(I)$) converged to a final $R = 0.0468$ and $wR = 0.0536$. TCNQ/$TCNQ^{\bullet-}$ are organized as tetrads and arranged in a helical fashion along the crystal b axis. The cations and TCNQ/$TCNQ^{\bullet-}$ form segregated stacks. Variable-temperature (77−303 K) electron spin resonance (ESR) data of single crystals and powders are presented. The powder ESR spectra of the complex salt have a temperature dependence typical of spin-coupled radical-pair systems. The separation energy (J) between the singlet ground state and triplet excited state is calculated to be 0.043 eV. The ESR signal line-width dependence on the single crystal orientation within the applied magnetic field requires a helical arrangement of the TCNQ/$TCNQ^{\bullet-}$ couples along the b axis as found in the X-ray study. When the temperature is lowered, the doublet (monoradical) signal experiences line broadening, and at 103 K the triplet transitions appear. The values of the D and E zero-field parameters are calculated to be 2.71×10^{-3} and 2.15×10^{-3} cm^{-1}, respectively. The complex salt has a resistivity typical of a semiconductor.

Introduction

The photochromism of spirooxazines (SO) was first reported by Fox[1] in 1961. These compounds are among the most interesting of functional dyes as they form deeply colored metastable merocyanine-type species (MC) upon exposure to ultraviolet light or heating (Scheme 1).

A large number of derivatives of the parent compound **1**, i.e., 1,3,3-trimethylspiro[indoline-2,3′-[3*H*]naphth[2,1-*b*][1,4]-oxazine], have been reported.[2] This family of compounds exhibits, with respect to photoexcitation, a durability higher than that of spiro[indolinenaphthopyrans],[3,4] a closely related class of photochromes in which a CH group has replaced the oxazine N1′ atom. The reported better fatigue resistance to photoaging has spurred intense research efforts aimed at assessing the potential of these photochromes in practical applications such as in recording, displaying, and copying materials, optical filters, special gadgets, etc.

Although the details of the photochemical processes involved in the photochromism[5−9] and reverse photochromism[10] of SOs are relatively well understood and theoretical calculations of the merocyanine isomeric distribution and of the SO and MC electronic absorption spectra have been reported,[11−14] only very limited data are presently available concerning the mechanism of spirooxazine photoaging. Indeed this class of photochromes after repeated exposure to dark−light cycles shows signs of remarkable photochemical fatigue that eventually results in a loss of their photochromic activity and therefore limits the application to mostly short- to medium-lasting systems.

Gautron et al.[15] was the first to identify the oxidation products of spiropyrans, and recently Guglielmetti and co-workers[16] have extended that study to spirooxazines. In the case of **1** the

* To whom correspondence should be addressed.

† Dedicated to K. U. Ingold on the occasion of his 65th birthday.

‡ Enichem Synthesis.

§ Present address: Great Lakes Chemical Italia S.r.l., Via Maritano 26, 20097 S. Donato (MI), Italy.

⊥ Eniricerche.

⊗ Abstract published in *Advance ACS Abstracts*, May 1, 1995.

(1) Fox, R. E. Research Report and Test Items Pertaining to Eye Protection of Air Crew Personnel. Final Report AD440226 on Contract AF41 (657)−215; Naval Research Lab, April 1961.

(2) Chu, N. Y. C. In *Photochromism: Molecules and Systems*; Durr, H., Bouas-Laurent, G., Eds.; Elsevier: Amsterdam, The Netherlands, 1990; pp 493−509.

(3) Chu, N. Y. C. *Can. J. Chem.* **1983**, *61*, 300−305.

(4) Chu, N. Y. C. *Sol. Energy Mater.* **1986**, *14*, 215−221.

(5) Albert, J. L.; Bertigny, J. P.; Aubard, J.; Dubest, R.; Dubois, J. E. *J. Chim. Phys. Phys.-Chim. Biol.* **1985**, *82*, 521−525.

(6) Schneider, S.; Mindl, A.; Elfinger, G.; Melzig, M. *Ber. Bunsen-Ges. Phys. Chem.* **1987**, *91*, 1222−1224.

(7) Schneider, S.; Baumann, F.; Kleuter, U.; Melzig, M. *Ber. Bunsen-Ges. Phys. Chem.* **1987**, *91*, 1225−1228.

(8) Aramaki, S.; Atkinson, G. H. *Chem. Phys. Lett.* **1990**, *170*, 181−186.

(9) Favaro, G.; Masetti, F.; Mazzucato, U.; Ottavi, G.; Allegrini, P.; Malatesta, V. *J. Chem. Soc., Faraday Trans.* **1994**, *90*, 333−338.

(10) Bohne, C.; Fan, M. G.; Li, Z.-J.; Yang, Y. C.; Lusztyk, J.; Scaiano, J. C. *J. Chem. Soc., Chem. Commun.* **1990**, 571−572.

(11) Malatesta, V.; Ranghino, G.; Allegrini, P.; Romano, U. *Int. J. Quantum Chem.* **1992**, *42*, 879−887.

(12) Malatesta, V.; Longo, L.; Fusco, R.; Marconi, G. *Mol. Cryst. Liq. Cryst.* **1994**, *246*, 235−236.

(13) Pottier, E.; Samat, A.; Guglielmetti, R.; Siri, R.; Pepe, G. *Bull. Soc. Chim. Belg.* **1992**, *101*, 307−310.

(14) Nakamura, S.; Uchida, K.; Murakami, A.; Irie, M. *J. Org. Chem.* **1993**, *58*, 5543−5545.

(15) Gautron, R. *Bull. Soc. Chim. Fr.* **1968**, *8*, 3190−3200, 3200−3204.

(16) Baillet, G.; Giusti, G.; Guglielmetti, R. *J. Photochem. Photobiol., A* **1993**, 157−161.

0002-7863/95/1517-6258$09.00/0

Scheme 1

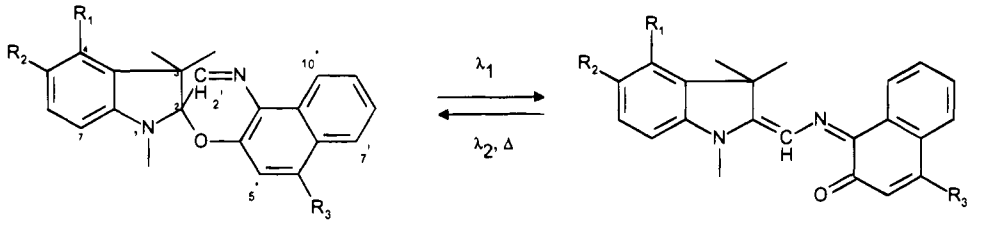

SO MC

1) $R_1 = R_2 = R_3 = H$;

2) $R_1 = R_2 = CH_3$; $R_3 = H$;

3) $R_1 = R_2 = H$; $R_3 =$ 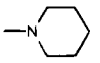

isolated major products were **4** and **5**. In those studies only

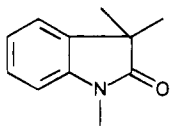

(4)

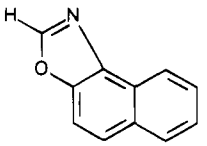

(5)

the structures of the final products were reported, and as no intermediate(s) in which the original indoline and naphthoxazine moieties are still linked together was isolated, it was not possible to elaborate on the details of the photodegradation which seems however to be, to a large extent, a light-promoted oxidation. The involvement of singlet O_2 ($^1\Delta_g$) that may form through the sensitizing action of the merocyanine forms has also been considered,[16] as well as the attack of ground-state molecular O_2 ($^3\Sigma_g$) on the diradicaloid species formed following the light-induced homolytic cleavage of the C2–O spiro bond. We have recently reported[17] that spirooxazines in either the closed SO or open MC forms not only are unable to promote the formation of singlet oxygen *via* photosensitization (*energy transfer*) processes but on the contrary behave as physical quenchers of this particularly reactive activated oxygen species. However, the demonstrated involvement of oxygen in the photodegradation of SOs has led us to suggest that an electron-transfer process from an excited state (most likely a triplet) of the merocyanine to ground-state molecular oxygen might trigger the (irreversible) oxidation process. We have proposed a mechanism in which the nucleophilic superoxide anion $O_2^{\bullet -}$ of the intermediate radical-ion pair ($MC^{\bullet +} \cdots O_2^{\bullet -}$) (Scheme 2) by attacking the

Scheme 2

$$SO \rightarrow MC \rightarrow (MC)^* \xrightarrow{O_2} MC^{\bullet +} \cdots O_2^{\bullet -}$$

electrophilic former C2 spiro carbon atom yields a diradical (**6**) that *via* cyclization to the carbon-centered oxazolyl radical and through a further electron and proton transfer gives **7** (route a, Scheme 3). The OH group of **7** must very likely derive from thermal or photochemical cleavage of a –O–OH group resulting from the peroxy –O–O$^\bullet$ radical by H atom abstraction from a suitable donor.

Compound **8** may then form in a reversible fashion from **7** by acidic treatment or, as we now know for the first time, directly from **1** through oxidative *dark reactions* that do not seem to require the involvement of molecular oxygen (route b, Scheme 3) but rather a mere electron transfer to an electron acceptor (EA). Indeed treatment of deaerated acetonitrile (ACN) solutions of **1** or **2**[18] with suitable electron acceptors such as, e.g., Cu(II) and Fe(III) ions, molecular iodine, tetracyanoethylene (TCNE), tetrachloro-1,4-benzoquinone (chloranil, CLA), or 7,7,8,8-tetracyanoquinodimethane (TCNQ) (**9**) directly yields

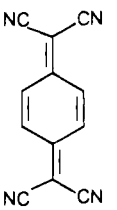

(9)

8. This novel finding is a rather important one mostly because in polymeric materials containing dispersed photochromic spiropyran or spirooxazine residual metal ions from polymerization catalysts, adventitious or deliberately added and potentially oxidizing organic species are usually present. These species may promote the photochrome irreversible oxidative degradation even under conditions of partial or total absence of oxygen as, e.g., in polymers coated with thin films of barrier agents such as SiO_2, SiO_xC_y, Al_2O_3, MgO, etc. This paper reports the synthesis and structural characterization of the first complex salt, i.e., TCNQ (**8b**)/$TCNQ^{\bullet -}$ (heretofore referred to as **8b**/$TCNQ_2^-$), that is formed by a dark reaction of spirooxazine **2** with TCNQ and has allowed us to unambiguously assign the structure of the oxidative degradation product of photochromic spirooxazines. The salt is paramagnetic and has a conductivity value typical of a semiconductor. Powder and single crystal electron spin resonance (ESR) investigations evidence the extensive delocalization of the $TCNQ^{\bullet -}$ ion-radical electron over tetrameric units (*tetrads*) formed by the TCNQ/$TCNQ^{\bullet -}$ species, with the cations being arranged in segregated layers nearly orthogonal to the TCNQ stacks. **1** and **3** undergo an analogous oxidative degradation.[18] However, so far we have not been able to obtain crystals suitable for the X-ray analysis, but NMR studies support structures **8a** and **8c** for the oxidation products of **1** and **3**, respectively.

Results and Discussion

A. Synthesis and Characterization. The thermal reaction between **2** and TCNQ (10^{-3} M; 1:2 ratio) in Ar-purged refluxing acetonitrile provides a complex salt, **8b**/$TCNQ_2^-$, that crystallizes as dark green platelets exhibiting semiconducting behavior (4×10^{-3} S cm^{-1}). The crystals are stable for prolonged periods

(17) Malatesta, V.; Milosa, M.; Millini, R.; Lanzini, L.; Bortolus, P.; Monti, S. *Mol. Cryst. Liq. Cryst.* **1994**, *246*, 303–310.

(18) Malatesta, V.; Wis, L. To be published.

Scheme 3

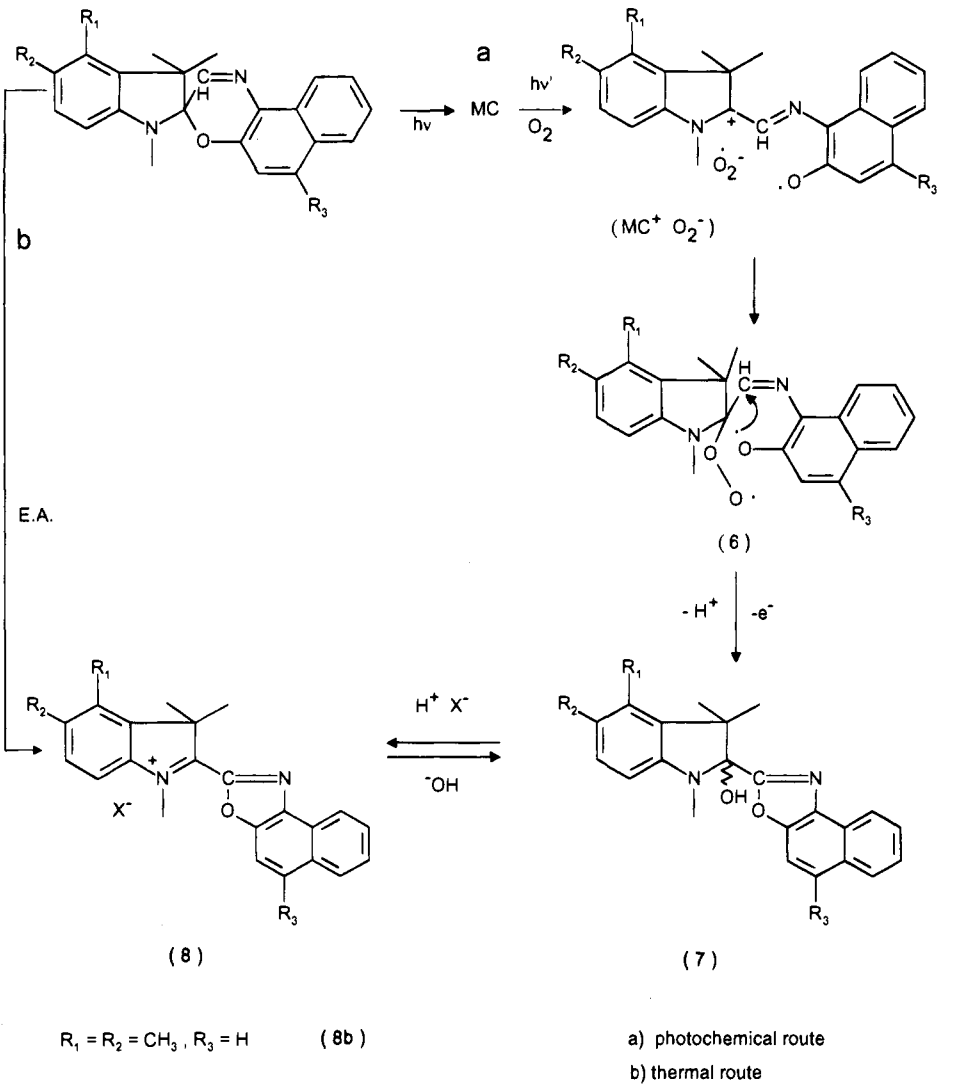

of time and in acetonitrile undergo a slow decomposition (30% after one month) when exposed to air. The highest peak in the electron impact (EI) mass spectrum of the complex salt corresponded to 340 ($M^+ - 15100$) with fragmentation peaks at lower mass, 186 (74) and 170 (81), due to the pentamethylindolium and naphthoxazolyl moieties, respectively.

Room temperature ^1H NMR spectra in DMSO-d_6 display a sharp singlet at 4.66 ppm due to the methyl group on the quaternary N atom shifted downfield with respect to that of NCH_3 observed in **2**.[19] Similarly all the ^{13}C NMR signals are shifted to lower fields except for C6, C5′, C9′, C10′, and C4′a. The former C2 spiro carbon atom resonance has moved to $\delta =$ 167.77 ppm from the original 99.29 ppm in **2** because of the presence of the −N=C2− double bond in **8b**. The methyl on N in the −N=C2− bond is also shifted downfield from the resonance value of the starting compound **2**, i.e., 37.92 vs 29.92 ppm. The observed NMR downfield shifts must originate from an extensive π-bond delocalization that requires a coplanarity of the indolium and naphthoxazolyl moieties as confirmed by the X-ray analysis (vide infra). Interestingly the NMR signals are sharp and do not seem to experience paramagnetic broadening by the $TCNQ^{\bullet-}$ radical anion, probably because extensive solvation of the ions favors solvent-separated ion pairs. The TCNQ ^1H and ^{13}C resonances were not observed probably because they are broadened beyond detection by a fast electron exchange among the TCNQ/$TCNQ^{\bullet-}$ species (vide infra). Elemental analysis gave a nominal stoichiometry of 1:1:1 for the complex salt **8b**/$TCNQ^{\bullet-}$/TCNQ. The IR stretching frequency of the CN group is 2178 cm^{-1}, and the peak is broad as found in other complex salts[20] whereas in neutral TCNQ the corresponding peak (2200 cm^{-1}) is very sharp. The nitrile peak is also sharp in simple salts such as, e.g., Li^+TCNQ^- and is shifted only 5 cm^{-1} (2195 cm^{-1}) with respect to neutral TCNQ.[20] $TCNQ_2^-$ (**8b**) is strongly fluorescent ($\lambda_{exc} = 430$ nm; $\lambda_{em} = 543$ nm).

B. X-ray Structure. The single crystal X-ray study confirmed the complex nature of the salt inferred from the elemental analysis results. The main crystallographic data and the bond lengths are reported in Tables 1 and 2, respectively. The asymmetric unit consists of one cation (**8b**) (Figure 1) and two TCNQ molecules (Figure 2). There are four asymmetric units per unit cell, i.e., four **8b** cations and, formally, four each of $TCNQ^{\bullet-}$ radical anions and TCNQ neutral molecules. In Figure 3 it is easy to identify groups of four TCNQ molecules (tetrads) made up of two independent A-type and B-type TCNQs stacked up in a ABB′A′/ABB′A′/etc. sequence, where the prime refers to molecules related to the one of the same kind in the first couple of the tetrad by an inversion symmetry operation. All the TCNQ molecules in a tetrad are stacked in a ring-over-bond overlap mode (Figure 2) with AB and BB′ distances of

(19) Malatesta, V.; Allegrini, P.; Neri, C.; Lanzini, L. *Magn. Reson. Chem.* **1992**, *30*, 905−908.

(20) Melby, R. J.; Harder, R. J.; Hertler, W. R.; Mahler, W.; Benson, R. E.; Mochel, W. E. *J. Am. Chem. Soc.* **1962**, *84*, 3374−3388.

Table 1. Experimental X-ray Data of **8b**/$TCNQ_2^-$

formula	$C_{48}H_{31}N_{10}O$
FW	763.84
T (K)	293
crystal system	monoclinic
space group	$P2_1/c$ (no. 14)
a (Å)	17.014 (3)
b (Å)	25.912 (5)
c (Å)	8.809(1)
β (deg)	90.18(1)
V (Å^3)	3883.6(11)
Z	4
D_{calcd} (Mg/m^3)	1.3064
diffractometer	Siemens AED
radiation (λ (Å))	Cu Kα (1.541 78)
scan type	$\pm h, k, l$
data collected	$\theta/2\theta$
θ range (deg)	3−65
F(000)	1588
μ(Cu Kα) (cm^{-1})	6.193
abs correction	no
std ref	200 every 100 measurements
no. of refl collected	7249
no. of unique refl	6853
R_{int}	0.0248
no. of refl obsd with $I > 3\sigma(I)$	4321
no. of variables	532
R	0.0468
wR	0.0536
S (goodness of fit)	1.573

Table 2. Bond Lengths (Å)[a]

N1−C2	1.307(4)	N1−C13	1.383(4)
C2−O3	1.376(4)	C2−C14	1.437(4)
O3−C4	1.372(4)	C4−C5	1.398(4)
C4−C13	1.383(5)	C5−C6	1.366(4)
C6−C7	1.428(5)	C7−C8	1.412(4)
C7−C12	1.422(4)	C8−C9	1.366(5)
C9−C10	1.392(4)	C10−C11	1.381(4)
C11−C12	1.403(5)	C12−C13	1.422(4)
C14−N15	1.308(4)	C14−C22	1.520(4)
N15−C16	1.432(4)	N15−C23	1.474(4)
C16−C17	1.382(4)	C16−C21	1.383(5)
C17−C18	1.377(4)	C18−C19	1.386(5)
C19−C20	1.414(4)	C19−C24	1.519(4)
C20−C21	1.396(4)	C20−C25	1.501(5)
C21−C22	1.527(4)	C22−C26	1.553(4)
C22−C27	1.524(5)	C28−C29	1.422(5)
C28−C33	1.433(5)	C28−C34	1.398(5)
C29−C30	1.354(5)	C30−C31	1.441(5)
C31−C32	1.418(5)	C31−C39	1.401(5)
C32−C33	1.361(5)	C34−C35	1.420(6)
C34−C37	1.420(5)	C35−N36	1.142(6)
C37−N38	1.147(5)	C39−C40	1.428(6)
C39−C42	1.422(6)	C40−N41	1.141(6)
C42−N43	1.165(6)	C44−C45	1.423(5)
C44−C49	1.436(4)	C44−C50	1.396(4)
C45−C46	1.369(5)	C46−C47	1.431(4)
C47−C48	1.423(5)	C47−C55	1.404(4)
C48−C49	1.358(4)	C50−C51	1.423(5)
C50−C53	1.420(4)	C51−N52	1.155(5)
C53−N54	1.143(5)	C55−C56	1.417(5)
C55−C58	1.413(4)	C56−N57	1.143(5)
C58−N59	1.160(5)		

[a] Estimated standard deviations are given in parentheses.

3.20 and 3.28 Å, respectively. The TCNQ B molecule is nearly planar while the A type is slightly bowed with the CN groups twisted out of plane of the outer −C=C− bonds. The mean angle between two TCNQ molecules is 3.7°. The tetrads are interrelated by a screw axis operation and form layers parallel to (100). The **8b** cations are completely planar and arranged between these stacks in a fish-bone-like pattern (Figure 4) and are nearly orthogonal to the TCNQ molecules, with the cation long axis making 116.5° and 113.5° angles with the type A and type B molecules, respectively. This type of segregated

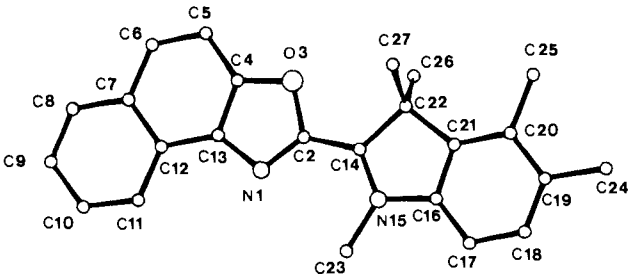

Figure 1. Atomic numbering of **8b**.

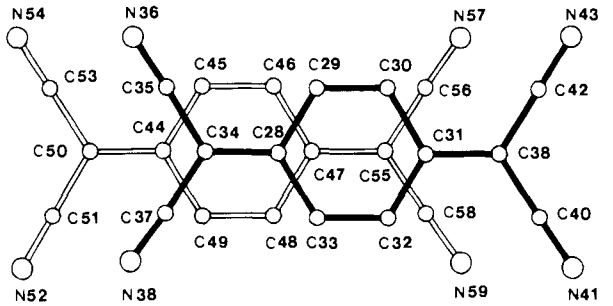

Figure 2. Nearest-neighboring packing and atomic numbering of TCNQ.

Chart 1. Mean Bond Lengths (Å) and Charges of TCNQ Molecules

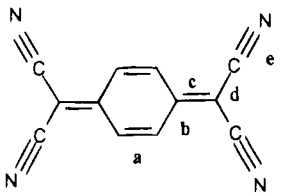

	a	b	c	d	e	δ*
TCNQ(A)	1.357	1.428	1.400	1.422	1.149	0.40
TCNQ(B)	1.363	1.428	1.400	1.424	1.150	0.38
$TCNQ^{0}$ [22a]	1.344	1.442	1.373	1.435	1.138	0.00
$TCNQ^{-}$ [22b]	1.363	1.442	1.420	1.417	1.145	1.00

* Negative charge calculated from the c−d and b−c bond length differences.[22]

stacks is unprecedented since all the reported TCNQ complex salts form either segregated or alternating stacks in which the two counterions are basically coplanar or lie in parallel planes.[21] The mean bond lengths of the independent TCNQ molecules are reported in Chart 1. By comparing these values with those observed for neutral and anionic TCNQ molecules, it is possible to estimate the amount of negative charge transfer and its distribution within the couples. Both molecules display rather similar mean bond lengths, which are intermediate between those of neutral TCNQ and $TCNQ^{\bullet-}$ anion radical. By applying the method of Flandrois and Chasseau,[22] based on the analysis of the bond length variation that is observed for TCNQ on going from the neutral to the anionic species, we estimate partial charges of $0.40e^-$ and $0.38e^-$ on the A- and B-type TCNQ molecules, respectively, these values being indicative of an extensive electron delocalization. The electron mobility could then account for the low resistivity displayed by **8b**/$TCNQ_2^-$ microcrystalline samples and for their peculiar paramagnetic properties.

C. ESR Study. The ESR powder spectra were recorded (1% in LiCl) in the temperature range 151−333 K, whereas

(21) Vogtle, F. *Supramolecular Chemistry*; Wiley: Chichester, U.K. 1991; pp 290−299.

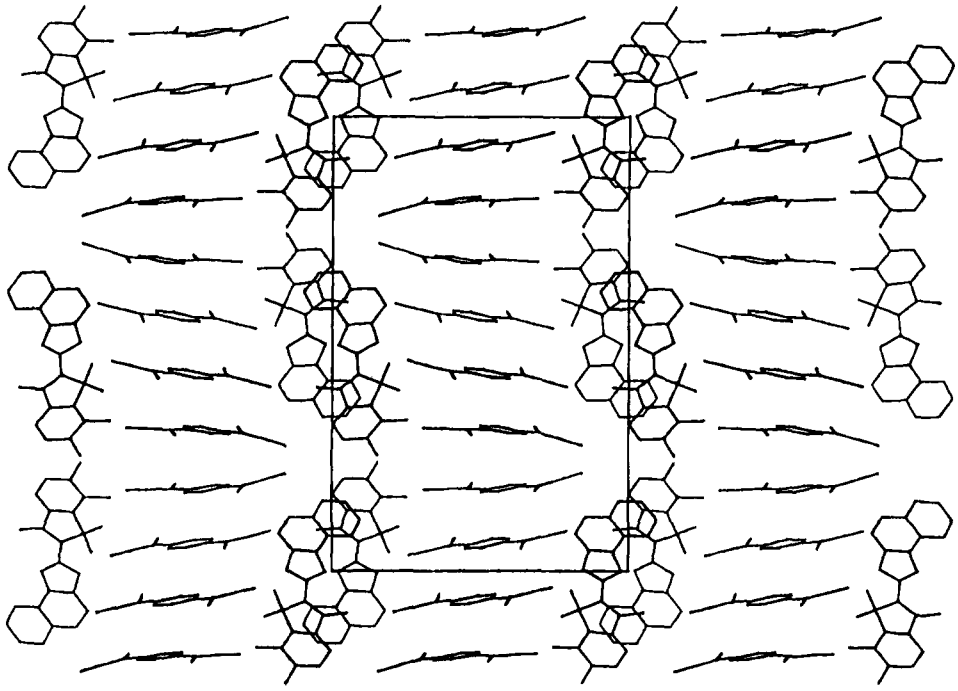

Figure 3. Crystal structure of **8b**/$TCNQ_2^-$ viewed along the *c* axis.

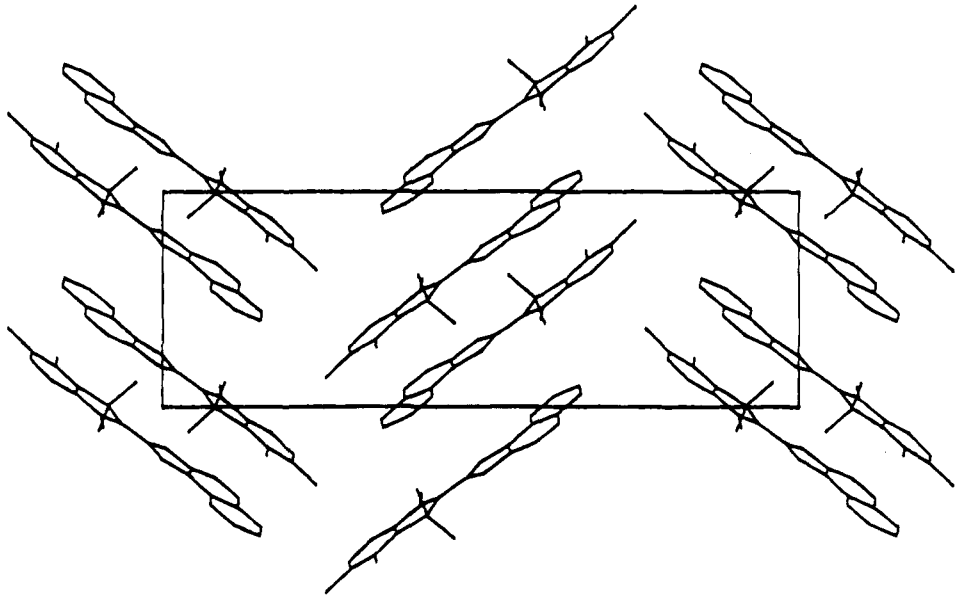

Figure 4. View of the fish-bone-like network of the **8b** cation in **8b**/$TCNQ_2^-$.

the single crystal ESR measurements were carried out at 298, 133, and 103 K. The temperature dependence of the integrated ESR signal can be fitted (Figure 5) to the expression

$$I = (1/T)(e^{J/KT} + 3)^{-1} \quad (1)$$

with a value of $J = 0.043$ eV, rather than to the simpler $1/T$ expression expected for an all-doublet-state system (monoradical). Equation 1 is characteristic of a coupled electron pair having a ground-state singlet and a thermally accessible triplet separated by the energy J. The lack of hyperfine splitting even at the lowest temperature (103 K) strongly suggests that the paramagnetic species is a mobile excited state (*triplet exciton*) and its motion is responsible for the averaging out of the electron–nucleus hyperfine interaction. Only below 103 K single crystals of **8b**/$TCNQ_2^-$ exhibit a doublet of lines from triplet excitons due to the $|\pm 1\rangle \leftrightarrow |0\rangle$ transitions. The spacing between the two lines is dependent on the crystal orientation within the external magnetic field (Figure 6). If one assumes

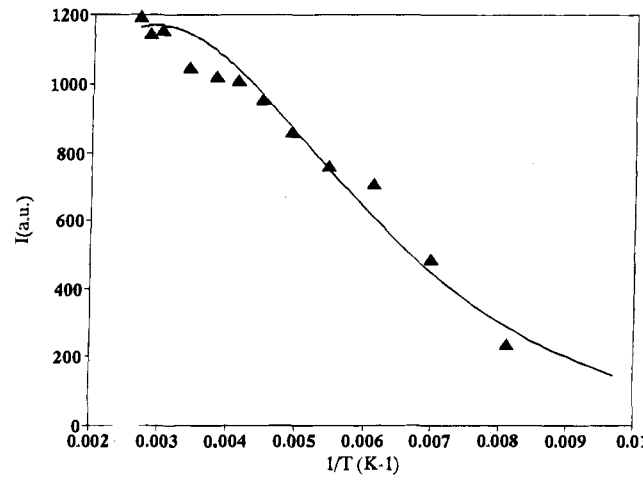

Figure 5. Temperature dependence of the integrated ESR absorption (I) (in arbitrary units) of **8b**/$TCNQ_2^-$.

Figure 6. Orientation dependence of the triplet splitting (outer lines) for an **8b**/$TCNQ_2^-$ single crystal. The orientation axis is indicated on each spectrum. The center line is assigned to the doublet (monoradical).

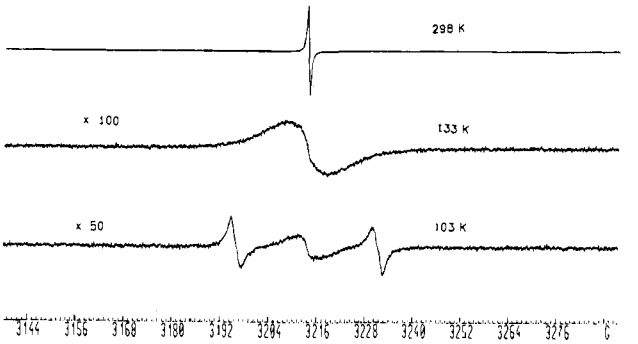

Figure 7. Temperature dependence of the ESR absorption of an **8b**/$TCNQ_2^-$ crystal at an arbitrary orientation. The spectra were obtained with different spectrometer settings at different temperatures.

that the doublet resonance arises from a zero-field splitting in a triplet state, the angular dependence of the doublet spacing is described by the spin Hamiltonian

$$H_s = g\beta BS + IAS + DS_z^2 + E(S_x^2 - S_y^2)$$

where $D = -(3/2)Z$ and $E = (-1/2)(X - Y)$. X, Y, and Z are the principal axis system of the electron spin−spin tensor, **A** is the hyperfine electron nucleus coupling tensor, I and S are the nuclear spin and the electron spin operators, respectively, and B is the magnetic field flux intensity. The calculated values for X, Y, and Z are −13, 32, and 19 G, and there is a substantial superimposition of the triplet species molecular axes with the crystallographic ones. The crystal field parameters D and E were calculated to be 2.71×10^{-3} and 2.15×10^{-3} cm^{-1}, respectively ($D/E = 1.3$). The D/E value deserves some comments as the magnitudes of D and E reflect the average spatial distribution of the correlated spins of the triplet exciton. Typically in the naphthalene and ethylene triplet state D/E is 7.3 and 0.9, respectively.[23] Usually the greater the two-dimensional extent of the molecular plane, the larger D will be with respect to E. The dipolar parameters of TCNQ are small relative to those of naphthalene ($D = 0.1006$ cm^{-1} and $E = 0.0138$ cm^{-1}), and this seems consistent with a model in which the triplet electrons encompass an extended π system which allows the effective distance of separation of the electrons to be larger than for naphthalene. Indeed from the maximum zero-field splitting (96 G) (Figure 6) it is possible to calculate[24] a "mean separation" for the two electrons of ca. 7 Å. This is in keeping with a model in which the triplet entity has a supramolecular distribution comprising at least two $TCNQ^{\bullet -}$ units whose electron pair gives a triplet delocalized over four TCNQ molecules (tetrad). The mean separation of 6.48 Å determined by X-ray study corresponds to the distance between the first and the third TCNQ molecule in a tetrad on the same stack. We have no evidence of the presence of coupled unpaired electrons located on different chains or stacks of TCNQ molecules. In this case we would observe additional resonance lines due to triplets from distant coupled unpaired electrons and having lower zero-field splitting (i.e., <96 G).[25] The forbidden $\Delta m_s = +2$ transition was not observed.

At room temperature the only detectable signal is that of the monoradical (Figure 7). Its line-width orientation dependence is shown in Figure 8 in the three *ab*, *ac*, and *bc* crystal planes. The observed angular dependence indicates that the rotation takes place in the molecular planes with the main line-width

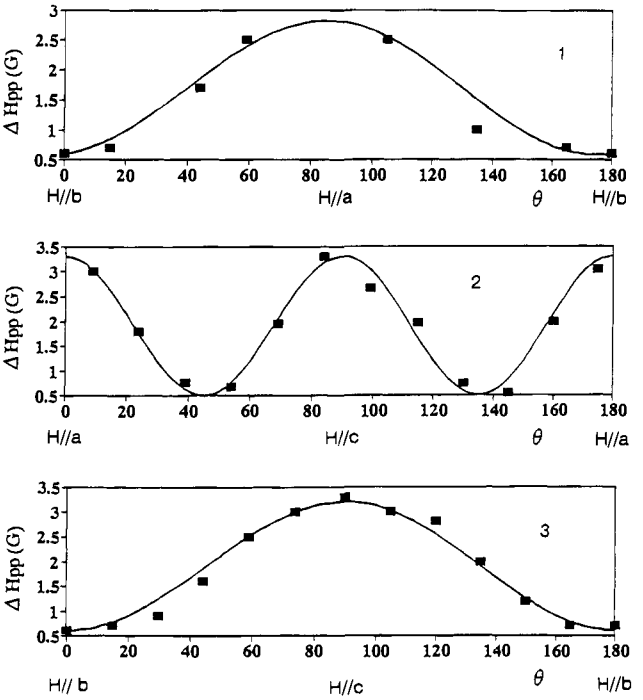

Figure 8. Line-width variation of the ESR signal of **8b**/$TCNQ_2^-$ at different orientations with respect to the magnetic field. The rotations 1, 2, and 3 are along the *c*, *b*, and *a* crystal axes, respectively.

values ΔH_{pp} being 3.4, 0.6, and 3.4 G along the *a*, *b*, and *c*, axes, respectively. It is worth noting that the periodicity in the *ac* plane is 90° rather than 180° as in the other two orthogonal planes. This behavior is a consequence of the helical arrangement of the four TCNQs within the tetrad that requires the same symmetry after a 90° rotation.

Conclusion

The results of our study suggest for the first time that the time-limited performance of photochromic spirooxazines might be due to their inherent proneness to become involved in irreversible electron-transfer processes to suitable and sometimes ubiquitous acceptors. As a consequence *dark reactions* that do not require oxygen may cause photochrome oxidative degradation and give products structurally related to those formed during the photoaging of these systems. In this respect the knowledge of the spirooxazine first-oxidation potential is deemed to be very important since it would enable one to calculate the amount of charge transfer to various acceptors[26] and rationalize their propensity to undergo oxidative degradation, and help in the

(22) (a) Flandrois, S.; Chasseau, D. *Acta Crystallogr.* **1977**, *B33*, 2744−2750. (b) Kistenmacher, T. J.; Enage, T. J.; Bloch, A. N.; Cowan, D. O. *Acta Crystallogr.* **1982**, *B38*, 1193−1197.

(23) Chesnut, D. B.; Phillips, W. D. *J. Chem. Phys.* **1961**, *35*, 1002−1012.

(24) Pake, G. E. *J. Chem. Phys.* **1948**, *16*, 327−335.

(25) Brown, I. M.; Jones, M. T. *J. Chem. Phys.* **1969**, *51*, 4687−4694.

(26) Wheland, R. C. *J. Am. Chem. Soc.* **1976**, *98*, 3926−3930.

molecular design of more stable spirooxazines. Electrochemical experiments are now in progress, and the results will be reported elsewhere.[27]

Experimental Section

General Methods. Infrared and electronic spectra were recorded on a Digilab FTS-15E and a HP 8452A or a Cary 2300 spectrometer, respectively. ^{1}H and ^{13}C NMR spectra were measured using a Bruker-300 AMX spectrometer. The assignments of the ^{1}H resonances were made by 2D nuclear Overhauser and exchange spectroscopy (NOESY) whereas distortionless enhancement by polarization transfer (DEPT) and two-dimensional heteronuclear correlation techniques were used for the mapping of ^{13}C chemical shifts. All chemical shifts are reported in parts per million (δ) relative to internal tetramethylsilane. Mass spectra were obtained on a Finnigan INCOS 50 mass spectrometer. The photochromes were synthesized in the Enichem Synthesis laboratories according to known literature methods.[2] Acetonitrile (Rudi-Pont HPLC grade) and 7,7,8,8-tetracyanoquinodimethane (Aldrich Co.) were used as received. The differential scanning calorimetry (DSC) analysis was carried out on a Mettler S30 calorimeter.

Preparation of Charge-Transfer Complex. To a solution of **2** (300 mg, 0.84 mmol) in deaerated ACN (200 mL) was slowly added (over 30 min) TCNQ (345 mg, 1.68 mmol) in ACN (200 mL) at room temperature. The mixture was refluxed for 2 h, cooled to ambient temperature, and left standing overnight. Dark green platelets with metallic luster (mp 203.3 °C dec) crystallized out of ACN solutions (34% isolated yield): ^{1}H NMR (300.13 MHz, DMSO-d_6) δ = 8.0 (H6), 7.6 (H7), 8.24 (H5′), 8.41 (H6′), 8.29 (H7′), 7.82 (H8′), 7.94 (H9′), 8.67 (H10′), 2.06 (*gem*-CH_3 at C3) 2.43 (CH_3 at C4), 2.54 (CH_3 at C5), 4.66 (NCH_3); ^{13}C NMR (75.47 MHz, DMSO-d_6) δ = 141.7 (C4), 133.28 (C5), 128.91 (C6), 130.47 (C7), 11.27 (C5′), 132.89 (C6′), 129.35 (C7′), 127.34 (C8′), 113.66 (C9′), 121.7 (C10′), 21.65 (*gem*-CH_3 at C3), 14.60 (CH_3 at C4), 19.55 (CH_3 at C5), 139.65 (C4a), 148.65 (C7a), 140.62 (C4′a), 37.92 (NCH_3), 54.79 (C3), 125.31 (C11′), 131.25 (C6′a), 136.60 (C10′a), 150.51 (OC=N$^-$), 167.77 (C=N$^+$); UV−vis (Cary 2300 spectrophotometer) λ_{max}(acetonitrile) = 460 nm (log ϵ = 4.39) (**8b**), 742 nm (log ϵ = 4.36) (TCNQ$^{\bullet-}$),[20] 840 nm (log ϵ = 4.65) (TCNQ$^{\bullet-}$);[20] FT-IR (Digilab FTS-15E spectrophotometer) 2178 cm^{-1} (br) (CN stretching); MS *m/e* (relative intensity) 340 (M^+ − 15100), 355 (M^+, 70), 186 (**74**, pentamethylindolium), 170 (81, naphthoxazolyl); Fluorescence (Aminco Bowman SL2) λ_{exc}(acetonitrile) = 430 nm, λ_{em} = 543 nm. The stoichiometry of the donor and acceptor was determined by elemental analysis. Anal. Calcd for $C_{48}H_{31}N_{10}O$: C, 75.47; H, 4.09; N, 18.34. Found: C, 75.51; H, 4.11; N, 18.28. Interestingly the same stoichiometry was observed[18] even when operating in the presence of large excess (up to 5:1) of TCNQ with respect to **2**.

Electrical Conductivity Measurements. Electrical conductivity was measured by using a four-probe method on a compressed pellet.

Crystal Structure Analysis. The X-ray diffraction data were collected by using a Siemens AED automated diffractometer with Cu Kα radiation monochromatized by graphite (λ = 1.5418 Å, $\theta/2\theta$ scans, θ_{max} = 65°). The structure was solved by direct methods by use of the SIR-88[28] program system and refined by the block-matrix least-squares method that uses the SHELX-76 softare package.[29] The function minimized was $\sum w(F_o - F_c)^2$ where $w^{-1} = \sigma^2(F) + 0.010709(F)^2$. The final cycles of refinement included atomic coordinates and anisotropic thermal parameters for all non-hydrogen atoms (532 parameters). Positions of H atoms were calculated on geometrical grounds and maintained fixed during the refinement, with U_{iso} = 0.06 Å^2 also being fixed. The final R factor was 0.0468 (wR = 0.0536) for all observed reflections with $I > 3\sigma(I)$. The difference Fourier map was featureless. The analysis of the molecular geometry has been carried out by using the PARST program.[30] Crystallographic data are given in Table 1. Bond lengths are listed in Table 2. The atomic numbering schemes are shown in Figures 1 and 2.

Electron Spin Resonance Studies. The measurement of electron spin resonance spectra was made with a Varian E109 spectrometer equipped with a 9 in. magnet. The crystal was glued on a heavy strip of paper which was then inserted snuggly in a 3 mm i.d. ESR quartz tube. The tube was mounted on a home-made goniometer that was inserted between the magnet pole expansion. The temperature was varied with a home-made temperature controller, over the 303−76 K range. The single crystal ESR spectra were recorded every 15° by rotating the crystal along its axes in the applied magnetic field. After a complete 180° rotation the same crystal was unglued and remounted along the other two remaining crystal axes, and the same analysis was repeated. The powder spectra were recorded on samples of the TCNQ ion complex salt diluted in LiCl (1% w/w) because of the very high signal intensity.

Acknowledgment. This work was funded and undertaken under the National Programme of Research for Chemistry sponsored by the Italian "Ministero per l'Universitá e la Ricerca Scientifica e Technologica" (Tema 10-Consorzio RCE). We thank Dr. M. Milosa for the preliminary experiments, Mr. G. Boara for the preparation of **8b**/$CuCl_2^-$ that was used as standard for the measurement of ϵ_{max} of **8b** and for helping with conductivity experiments, and Dr. P. Allegrini for providing us with a sample of **2**.

Supplementary Material Available: Tables listing fractional atomic coordinates, isotropic equivalent thermal parameters, anisotropic thermal parameters, calculated fractional coordinates for H atoms, bond angles, torsion angles, and mean plane equations (9 pages); table listing observed and calculated structure factors (25 pages). This material is contained in many libraries on microfiche, immediately follows this article in the microfilm version of the journal, can be ordered from the ACS, and can be downloaded from the Internet; see any current masthead page for ordering information and Internet access instructions.

JA9421718

(27) The first redox potential of TCNQ, TCNE, and CLA is 220, 240, and 20 mV vs SCE (ACN, $LiClO_4$, 0.1 M),[18] respectively. In preliminary experiments no oxidation wave has been observed for **2** and **3** even at the fastest potential scanning rate (100 V/s). This behavior might suggest that the transients from the first and second electron transfer are too short lived to be observed under our experimental conditions. However, the spirooxazine first oxidation potential must be <20 mV.

(28) Burla, M. C.; Camalli, M.; Cascarano, G.; Giacovazzo, C.; Polidori, G.; Spagna, R.; Viterbo, R. *J. Appl. Crystallogr.* **1989**, *22*, 389−393.
(29) Sheldrick, G. M. *SHELIX: A program for Crystal Structure Determination*; University of Cambridge: Cambridge, England, 1976.
(30) Nardelli, M. *Comput. Chem.* **1983**, *7*, 95−98.